Molecular Therapy
Original Article

Dominant-Negative TGF-β Receptor Enhances PSMA-Targeted Human CAR T Cell Proliferation And Augments Prostate Cancer Eradication

Christopher C. Kloss,[1,4] Jihyun Lee,[1,5] Aaron Zhang,[1] Fang Chen,[1] Jan Joseph Melenhorst,[1,2,3] Simon F. Lacey,[1] Marcela V. Maus,[1,6] Joseph A. Fraietta,[1,2,3] Yangbing Zhao,[1,2] and Carl H. June[1,2,3,4]

[1]Center for Cellular Immunotherapies, Perelman School of Medicine, University of Pennsylvania, Philadelphia, PA 19104-5156, USA; [2]Department of Pathology and Laboratory Medicine, Perelman School of Medicine, University of Pennsylvania, Philadelphia, PA 19104-5156, USA; [3]Parker Institute for Cancer at the University of Pennsylvania, Philadelphia, PA 19104-5156, USA; [4]Smilow Center for Translational Research, 3400 Civic Center Blvd., Philadelphia, PA 19104-5156, USA

Cancer has an impressive ability to evolve multiple processes to evade therapies. While immunotherapies and vaccines have shown great promise, particularly in certain solid tumors such as prostate cancer, they have been met with resistance from tumors that use a multitude of mechanisms of immunosuppression to limit effectiveness. Prostate cancer, in particular, secretes transforming growth factor β (TGF-β) as a means to inhibit immunity while allowing for cancer progression. Blocking TGF-β signaling in T cells increases their ability to infiltrate, proliferate, and mediate antitumor responses in prostate cancer models. We tested whether the potency of chimeric antigen receptor (CAR) T cells directed to prostate-specific membrane antigen (PSMA) could be enhanced by the co-expression of a dominant-negative TGF-βRII (dnTGF-βRII). Upon expression of the dominant-negative TGF-βRII in CAR T cells, we observed increased proliferation of these lymphocytes, enhanced cytokine secretion, resistance to exhaustion, long-term *in vivo* persistence, and the induction of tumor eradication in aggressive human prostate cancer mouse models. Based on our observations, we initiated a phase I clinical trial to assess these CAR T cells as a novel approach for patients with relapsed and refractory metastatic prostate cancer (ClinicalTrials.gov: NCT03089203).

INTRODUCTION

Prostate cancer is the most common and second most deadly cancer for men. Upon metastasis to bone, the disease usually becomes refractory to therapy and often results in death within 3–5 years.[1] Metastatic prostate cancer is minimally responsive to checkpoint blockade of PD-1 and CTLA-4.[2]

The recent medical breakthroughs of cancer immunotherapy have demonstrated the power that harnessing the immune system can have to eliminate cancer cells.[3] Most of these therapies rely on the triggering of immune responses upon administering monoclonal antibodies that block various immunosuppressive signals.[4,5] However, relying on endogenous responses makes it difficult to achieve high therapeutic efficacy while avoiding toxic autoimmune side effects.[6]

For more precise therapy, T cells can be engineered with chimeric antigen receptor (CAR) constructs to recognize and exert cytotoxic effects on cells expressing specific antigens.[7,8] A challenge to the success of these therapies is the immunosuppressive microenvironment that re-directed T cells encounter upon infiltration into the tumor bed.[9,10]

To achieve therapeutic success within solid tumors, CAR T cells need to overcome immunosuppressive signals. One approach is to block immunosuppressive pathways such as PD-1 and/or CTLA-4 in combination with CAR T cells to achieve an enhanced response.[11,12] Many cancers, particularly prostate cancer, are known to secrete transforming growth factor β (TGF-β), creating an immunosuppressive milieu. TGF-β is known to induce or promote metastasis and neoangiogenesis and to potently suppress the immune system.[13–15] Studies in the 1990s demonstrated that TGF-β signaling can be blocked by using a dominant-negative TGFBRII (dnTGF-βRII), which is truncated and lacks the intracellular domain necessary for downstream signaling.[16,17] Expression of the dnTGF-βRII enhances antitumor immunity and can lead to autoimmunity.[18,19] Furthermore, transgenic mice expressing dnTGF-βRII develop a lymphoproliferative disorder.[20] Two studies demonstrated enhanced T cell infiltration into tumors with potent antitumor responses in the transgenic adenocarcinoma mouse prostate (TRAMP) mouse model of prostate cancer when utilizing this receptor.[21,22] A clinical trial (ClinicalTrials.gov: NCT00368082) testing the safety and efficacy of the dnTGF-βRII receptor in Epstein-Barr virus (EBV)-specific T cells for lymphoma was recently reported.[23,24]

Received 13 January 2018; accepted 4 May 2018;
https://doi.org/10.1016/j.ymthe.2018.05.003.

[5]Present address: LG Chem, Ltd., Seoul, South Korea

[6]Present address: Massachusetts General Hospital, Boston, MA 02114, USA

Correspondence: Christopher C. Kloss, Smilow Center for Translational Research, 3400 Civic Center Blvd., Philadelphia, PA 19104-5156, USA.
E-mail: klosschr@pennmedicine.upenn.edu

Correspondence: Carl H. June, Smilow Center for Translational Research, 3400 Civic Center Blvd., Philadelphia, PA 19104-5156, USA.
E-mail: cjune@upenn.edu

Glutamate carboxypeptidase II or prostate-specific membrane antigen (PSMA) is a type II membrane glycoprotein that has been studied within the prostate cancer field for three decades as a tumor-associated antigen for prostate cancer. There is low-level expression in some normal tissues (e.g., astrocytes, neurons, kidney epithelium, and salivary gland). Many methodologies use PSMA either for positron emission tomography (PET) imaging or for antibody-targeted therapies.[25] In addition, a trial has been open since 2010 using anti-PSMA CAR T cells employing a CD28 costimulatory and CD3ζ activation domain with reported limited persistence of the CAR T cells and no observed responses (ClinicalTrials.gov: NCT01140373), indicating a need for a more potent PSMA-specific CAR T cell.

We reasoned that co-expressing the dnTGF-βRII with a PSMA-specific CAR in T cells would result in enhanced infiltration, proliferation, persistence, and efficacy when treating prostate cancer. We characterized the mechanisms underlying the potency-enhancing effects of TGF-β blockade in anti-PSMA Pbbz CAR T cells.

RESULTS

The design of the CARs used in these studies is described in the Materials and Methods. All CARs used the 4-1BB costimulatory and CD3ζ-signaling domains that are in tisagenlecleucel, the CAR recently approved by the U.S. Food and Drug Administration for leukemia. Employing lentiviral vectors, we routinely obtain 30%–60% transduction efficiencies of primary human T cells using an MOI of 1 to 2. Mock-transduced cells were included to control for allogeneic effects. A mismatched CAR was included that targets CD19 (tisagenlecleucel, 19BBZ) to control for antigen-independent effects of the CAR components. In the case of the anti-PSMA CAR (Pbbz), the scFv was derived from the mouse J591 monoclonal antibody that had been previously humanized.[26]

Utilizing a T2A element, we obtained efficient co-expression of the dnTGF-βRII with the Pbbz CAR (dnTGF-βRII-T2A-Pbbz (Figure 1A). This dnTGF-βRII functions to block TGF-β signaling, which was demonstrated by differential SMAD2/3 phosphorylation in CAR-positive and CAR-negative cells upon stimulation with human TGF-β (Figure 1B). The Pbbz CAR functioned to induce specific lysis of human prostate cancer cells only when they expressed PSMA (Figure 1C). The PC3 prostate cancer cell line was verified to secrete high levels of latent TGF-β (Figure 1D). When these PC3-PSMA$^+$ tumor cells were used for long-term co-culture experiments with Pbbz CAR T cells, the CAR T cells co-expressing the dnTGF-βRII had a much higher population doubling observed, with ∼15-fold higher proliferation over 42 days co-culture and repetitive stimulation with PSMA-expressing tumor cells (Figure 1E). This enhanced proliferation was antigen dependent, because it was not observed in cultures of CAR T cells with or without tumor cells that did not express PSMA (Figure 1E, top panels).

Intrigued by the ability of dnTGF-βRII-T2A-Pbbz CAR T cells to proliferate more efficiently than Pbbz alone in the presence of tumor cells that secrete TGF-β, we next interrogated these *in vitro* co-cultures more closely. At days 0, 7, 14, 21, and 28, we harvested the T cells and supernatant for analyses. The CD8+ T cell percentage declined from the routinely obtained 30% at baseline to 7.8% in Pbbz and 5.0% in dnTGF-βRII-T2A-Pbbz by day 28. There was a modest increase from 1.56% to 3.55% of CD4+ CAR T cells that expressed CD127. We found that there was a statistically higher percentage of central memory CD8$^+$ T cells with a significant loss of FoxP3 staining from 38% in Pbbz to 25% in dnTGF-βRII-T2A-Pbbz (Figures 2A and 2B). From cytokine analysis, we determined that T_H2 cytokines (i.e., interleukin-4 [IL-4], IL-5, and IL-13) were differentially secreted at higher amounts in dnTGF-βRII-T2A-Pbbz than in Pbbz (Figure 2C). IL-2 secretion by the PSMA Pbbz CAR T cells was similar with or without dnTGF-βRII. In addition, the innate immune cell-recruiting cytokines IP-10, MIP1-α, MIP1-β, and RANTES were elevated in the dnTGF-βRII-T2A-Pbbz group compared to the Pbbz group.

By harvesting total mRNA from these T cells at spaced time intervals after the initiation of culture, we performed longitudinal whole-transcriptome and microRNA microarray analysis. Interestingly, at 7 days of co-culture with PC3-PSMA, these dnTGF-βRII-T2A-Pbbz T cells only had 16 differentially expressed (>2- or <−2-fold change) genes or microRNAs (Table S1). Most of these were either unannotated genes or microRNAs. After 14 days, there were 51 differentially expressed genes or microRNAs. Finally, after 21 days there were 343 differentially expressed genes or microRNAs. Confirmed by cytokine analysis, IL-4, IL-5, and IL-13 were among the highest differentially expressed genes (DEGs) in the dnTGF-βRII-T2A-Pbbz group. Other highly DEGs of interest included EOMES, IFNG, PTGDR2, EPAS1, EGR1, and ARG2 (Figure S1; Table S1).

A protein-protein interaction (PPI) network was constructed using the DEGs on days 14 and 21 of co-culture with the PC3-PSMA tumor cells (Figure 3). The PPI was constructed using STRING.[27] On day 14, the analysis shown in Figure 3A indicates that more inter-protein interactions were found than expected by random interaction ($p < 1.3 \times 10^{-14}$). There were 3 clusters of proteins preferentially interacting in dnTGF-βRII-T2A-Pbbz PSMA CAR T cells on day 14. One cluster comprised cytokine-related proteins (IL-4, IL-5, SOCS1, IL-23R, PTGDR2, TLR7, etc.), another comprised transcription factors (FOS, FOSL2, EGR1, JUN, JUNB, and JUND), and the last, hypoxia-related factors (ARNT, EGLN3, and EPAS1). In contrast, on day 21 there were 2 main clusters of predicted functional or structural PPIs (Figure 3B): one comprised cell cycle-related proteins (CCNA1, CCNA2, CCNB1, CCNB2, CDK1, CDC20, CDC20B, CDC45, CKS, CKS1B, and TP73), and the other, cytokines and chemokines (leukemia inhibitory factor [LIF], interferon [IFN]-γ, IL-1A, IL-3RA, IL-4, IL-5, colony-stimulating factor 2 [CSF2], oncostatin M [OSM], IL-13, and CCL3).

The DEGs were then mapped to the Kyoto Encyclopedia of Genes and Genomes (KEGG) pathways, and their enrichment for specific pathways was investigated using STRING analysis. On day 21, there were 24 KEGG pathways identified, including cell signaling (cytokine

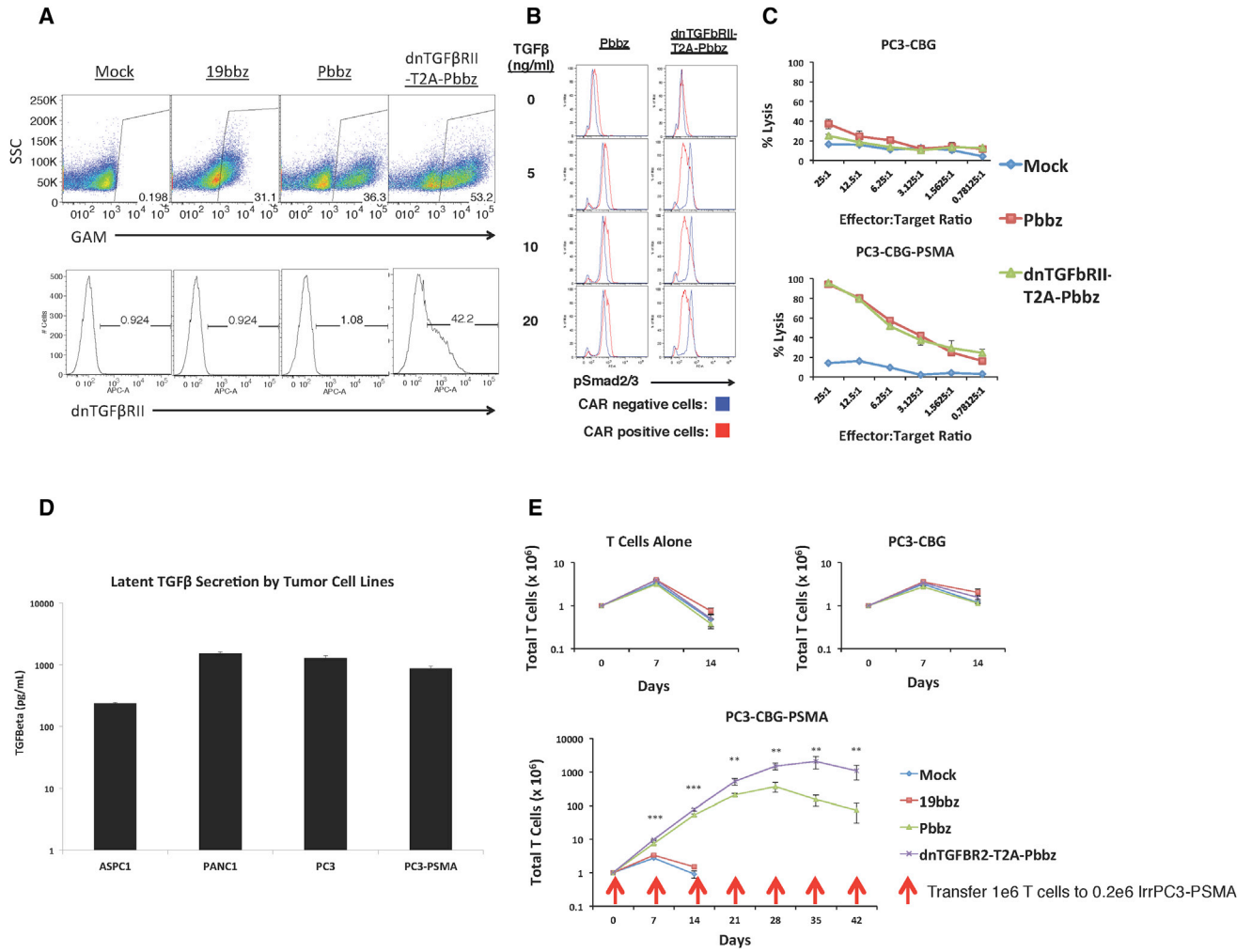

Figure 1. *In Vitro* Functionality of Pbbz CAR and dnTGF-βRII-T2A-Pbbz CAR

(A) Lentiviral transduction allows for efficient expression of 19bbz, Pbbz alone, or dnTGF-βRII-T2A-Pbbz in primary human T cells. (B) Expression of dnTGF-βRII prevents TGF-β signal induction through Smad2/3. (C) T cells expressing Pbbz specifically lyse PSMA$^+$ PC3 cells in 24-hr luciferase-based lysis assays. (D) ELISA determination of the secretion of the latent form of TGF-β by tumor lines. (E) Expression of dnTGF-βRII-T2A-Pbbz enhances antigen-specific proliferation of CAR T cells upon co-culture with PSMA$^+$ PC3 cells (y axis log10 scale). The error bars represent ± SD. **$p < 0.01$, and ***$p < 0.001$.

interactions, Jak-STAT, cell cycle, TCR signaling, and FcεR1 signaling) and autoimmunity (inflammatory bowel disease, rheumatoid arthritis, systemic lupus erythematosus, and type I diabetes) that were statistically significant associations (false discovery rates for all <0.005) (Table S2). The KEGG pathways identified on day 14 were similar. Finally, we also used the DEG to conduct gene ontology (GO) analysis. There were many biologic processes identified; the top 10 are shown in Table 1 and the entire list is shown in Table S3. The top GO terms identified on day 14 were biologic processes primarily related to effector immune responses, and on day 21, GO terms were related to cell cycle and cell division.

From these robust *in vitro* results, we postulated that the dnTGF-βRII-T2A-Pbbz CAR T cells had more sustained effector functions in the presence of tumor cells that express TGF-β than the CAR alone, based on the enhanced cytokine and cell cycle gene expression data. To test this hypothesis *in vivo*, we infused the PC3-PSMA human prostate cancer cells into NOD/SCID IL-2gamma (NSG) mice, allowing disseminated tumors to form in the mice within the lung, liver, bone, kidney, stomach, pancreas, head, and spinal cord. In this model, the mice died 4–6 weeks following tumor injection. The PC3-PSMA cells were engineered to express luciferase, allowing tumor burden to be easily quantified. After allowing these tumors to engraft and disseminate for 2 weeks, we infused 5×10^6 CAR T cells by tail vein (Figure 4A). It is evident from the tumor burden quantification that the dnTGF-βRII-T2A-Pbbz CAR T cells functioned significantly better than Pbbz CAR T cells alone and eradicated the tumor from these mice (Figure 4B). The images confirm that

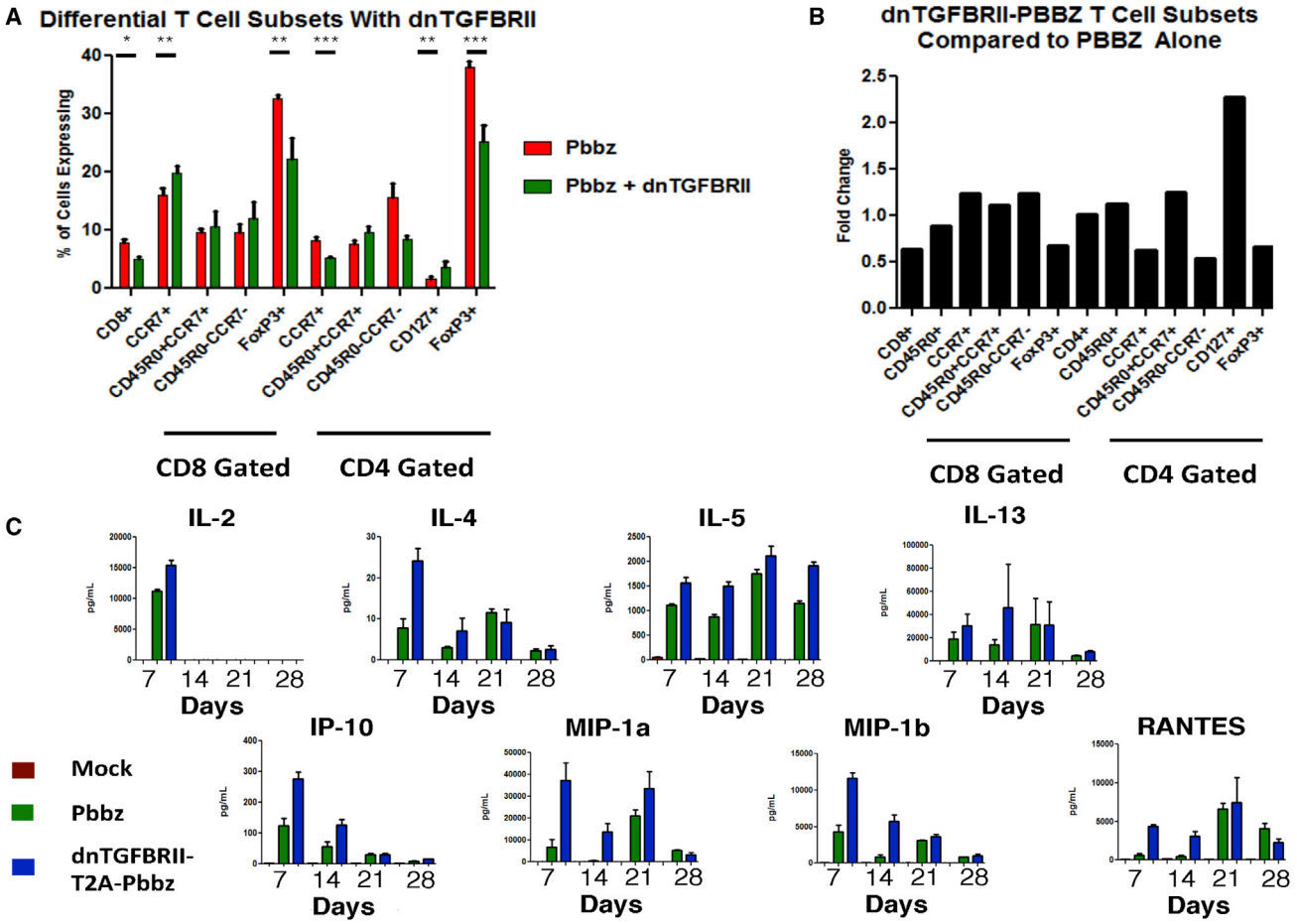

Figure 2. Flow Cytometric and Multiplex Cytokine Profiling of CAR T Cell Subsets from PC3-PSMA Co-culture

(A and B) T cells were analyzed with flow cytometry at day 21 post co-culture of Pbbz or dnTGF-βRII-T2A-Pbbz CAR T cells. (A) shows the differential percentage of various T cell subsets, which is further represented as fold change of T cell subsets found in the dnTGF-βRII-T2A-Pbbz versus Pbbz CAR T cells alone (B). (C) Luminex 30-Plex cytokine analysis was performed using T cell supernatants isolated at days 7, 14, 21, and 28 from Pbbz or dnTGF-βRII-T2A-Pbbz CAR T cells, as shown in Figure 1E. Pbbz-alone T cells, green bars; dnTGF-βRII-T2A-Pbbz T cells, blue bars. The error bars represent ± SD. *$p < 0.05$, **$p < 0.01$, and ***$p < 0.001$.

the dnTGF-βRII-T2A-Pbbz CAR T cells eliminated tumor in 4/4 mice, while the Pbbz T cells alone allowed for only 1/4 mice to achieve eradication (Figure 4C). In contrast all mice in the mock T cell group died from tumor progression 21–28 days after T cell injection. Interestingly, the levels of human T cells in the dnTGF-βRII-T2A-Pbbz group were 7 times higher in blood than the levels of Pbbz T cells, and 85% of these cells were $CD4^+$ CAR T cells (Figure 4D). In addition, the tumor-free mice in the dnTGF-βRII-T2A-Pbbz group began to have weight loss and developed signs of xenogeneic graft-versus-host disease (GVHD) (xGVHD), requiring euthanasia a month after CAR T cell infusion.

To further compare the CAR T cells *in vivo*, we used the PC3-PSMA NSG mouse metastatic prostate cancer model to perform a dose escalation trial of dnTGF-βRII-T2A-Pbbz PSMA CAR and Pbbz PSMA CAR T cells. At 2 weeks following tumor injection, doses of 0.5×10^6 and 2.5×10^6 CAR T cells were infused intravenously (i.v.) (Figure 5A); note that the dose used in the first experiment was 5×10^6 CAR T cells. In this experiment, we observed that the higher dose of dnTGF-βRII-T2A-Pbbz CAR T cells caused regression of tumor burden at day 14, while mice in the mock and CD19 CAR T cell control groups had progressive tumor burdens that required sacrifice according to predetermined endpoints of the protocol (Figure 5B). By day 42, 4/5 mice treated with PSMA dnTGF-βRII-T2A-Pbbz CAR T cells had tumor eradication (Figure 5D). In contrast, the mice given the lower dose of dnTGF-βRII-T2A-Pbbz CAR T cells had initial tumor control until day 21, followed by tumor relapse similar to the mice treated with PSMA Pbbz CAR T cells.

Intriguingly, the mice treated with the higher dose of dnTGF-βRII-T2A-Pbbz CAR T cells had a significant loss of body weight between days 28 and 35, but then they recovered to previous weight by day 42 following tumor elimination (Figure 5C). The mechanism of the reversible weight loss is not known, but it may be

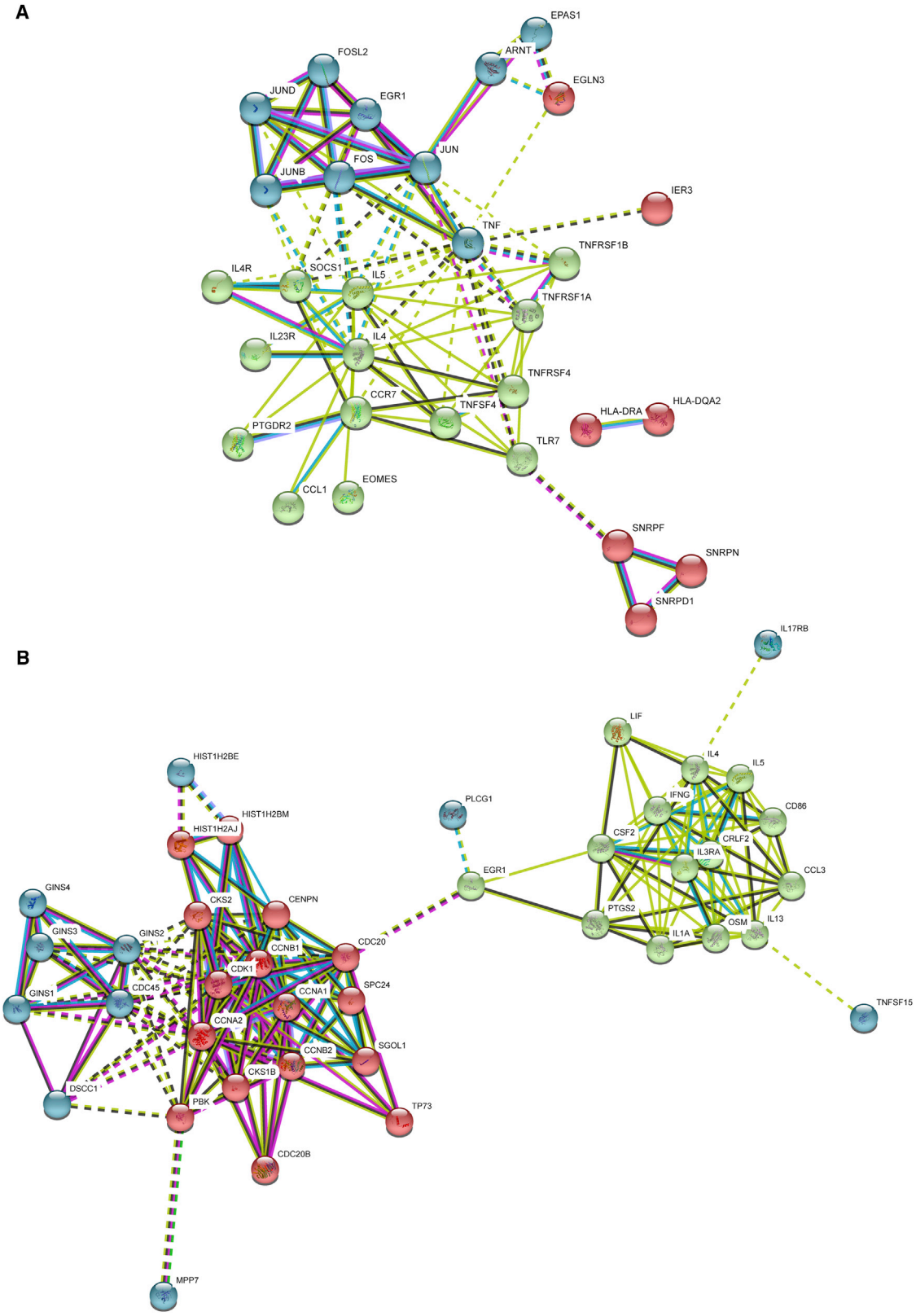

(legend on next page)

Table 1. Pathway Analysis Showing Over-representation of Gene Ontology Biological Process Terms Related to Inflammation and Cell Cycle in dnTGF-βRII-T2A-Pbbz PSMA CAR T Cells at Days 14 and 21 of Culture

Pathway ID	Pathway Description	Observed Gene Count	False Discovery Rate
Day 14			
GO.0034097	response to cytokine	14	8.87E−08
GO.0051707	response to other organism	14	8.87E−08
GO.1903708	positive regulation of hemopoiesis	9	9.32E−08
GO.1902107	positive regulation of leukocyte differentiation	8	4.32E−07
GO.0033993	response to lipid	13	3.61E−06
GO.0032496	response to lipopolysaccharide	9	5.37E−06
GO.0002639	positive regulation of immunoglobulin production	5	5.66E−06
GO.0006954	inflammatory response	10	1.01E−05
GO.0031347	regulation of defense response	12	1.19E−05
GO.0009617	response to bacterium	10	1.44E−05
Day 21			
GO.0000278	mitotic cell cycle	67	2.00E−34
GO.1903047	mitotic cell cycle process	57	1.46E−27
GO.0007049	cell cycle	72	7.91E−27
GO.0022402	cell cycle process	62	1.12E−24
GO.0007067	mitotic nuclear division	39	6.56E−24
GO.0051301	cell division	42	8.18E−22
GO.0000280	nuclear division	40	1.50E−21
GO.0048285	organelle fission	41	1.50E−21
GO.0007059	chromosome segregation	27	1.62E−18
GO.0051726	regulation of cell cycle	45	2.17E−13

The top 10 processes are listed; the complete list is shown in Table S3.

related to cytokine release. It is also possible that the weight loss was related to overexpression of LIF in the dnTGF-βRII-T2A-Pbbz CAR T cells,[28] a gene with >4-fold higher expression than in Pbbz CAR T cells with intact TGF signaling (Table S1). As in the first experiment, there were elevated levels of human CAR T cells found in the blood at days 33 and 64 in the high-dose dnTGF-βRII-T2A-Pbbz CAR T cell group, with associated signs of xGVHD at day 64 (Figure 5E).

To further determine mechanisms leading to enhanced proliferation and antitumor efficacy of CAR T cells that are expressing the dnTGF-βRII, we performed an additional *in vivo* experiment to investigate the effects of the dnTGF-βRII on T cell differentiation. Mice were randomized to T cell treatment groups within the same cage of mice to control for unforeseen variables affecting T cell engraftment and proliferation, weight loss, and GVHD. Using a protocol like that shown in Figure 4, mice were injected with 5×10^6 CAR T cells, and we included 10 mice per group in anticipation of needing to sacrifice animals to necropsy to investigate the GVHD (Figure 6A). Similar to the previous animal experiments, the dnTGF-βRII-T2A-Pbbz group had superior antitumor efficacy and controlled the tumors long-term, while the Pbbz group exhibited progressive cancer (Figures 6B and 6D).

Similar to the previous animal experiments, the dnTGF-βRII-T2A-Pbbz group had progressive weight loss and developed signs of xGVHD around day 35, with all of the mice requiring euthanasia at approximately day 42 (Figure 6C). Confirming previous experiments, there was a striking enhancement of CAR T cells in the dnTGF-βRII-T2A-Pbbz group of mice, as the mouse blood at day 35 contained approximately 25×10^6 human CAR T cells per mL of mouse blood compared to less than 1e6 CAR T cells per mL in the Pbbz T cell group. The CAR T cell lymphocytosis comprised both CD4+ and CD8+ T cells, with approximately a 2:1 CD4:CD8 ratio on day 35. Importantly, we found that the dnTGF-βRII-T2A-Pbbz mice had significantly higher levels of central memory $CD8^+$ T cells (Figure 6E). We did not observe any difference in the numbers of $FoxP3^+$ T cells within the blood of these mice.

DISCUSSION

Our results indicate that PSMA-specific, TGF-β-insensitive (dnTGF-βRII-T2A-Pbbz) CAR T cells can specifically eliminate advanced tumors that express PSMA. In addition, the PSMA-specific, TGF-β-insensitive CAR T cells have a striking proliferative advantage over wild-type PSMA CAR T cells that retain TGF-β signaling. These results have potential clinical utility, because all reported CAR T cell trials to date in patients with solid tumors have had disappointing CAR T cell expansion[7,8] that is several orders of magnitude that below CD19- and BCMA-specific CAR T cells employed for hematologic malignancies.[29,30]

From these long-term *in vitro* proliferation assays, we used multiple modalities to further characterize and interrogate the mechanisms for this enhanced proliferation upon TGF-β blockade. Most interestingly, we identified a distinct transcriptional program in the T cells expressing PSMA Pbbz CAR and the dnTGF-βRII-T2A-Pbbz CAR in the presence of TGF-β, as there were 329 genes or microRNAs (miRNAs) that were differentially expressed by >2-fold after 21 days of culture.

The dnTGF-βRII-T2A-Pbbz CAR T cells have enhanced cytokine signaling and secretion of a variety of cytokines that would be

Figure 3. Protein-Protein Interactions in PSMA dnTGF-βRII-T2A-Pbbz CAR T Cells

A protein-protein interaction network was constructed using STRING, version 10.5, based on differentially expressed genes on days 14 (A) and 21 (B) of culture. Network nodes represent proteins and the edges represent protein-protein interactions (physical or functional). In (A), the network has 43 nodes and 91 edges, with a p value of 1.3×10^{-14} compared to random interactions. In (B), the network has 69 nodes and 182 edges, with a p value of $<1.0 \times 10^{-16}$ compared to random interactions. The error bars represent ± SD.

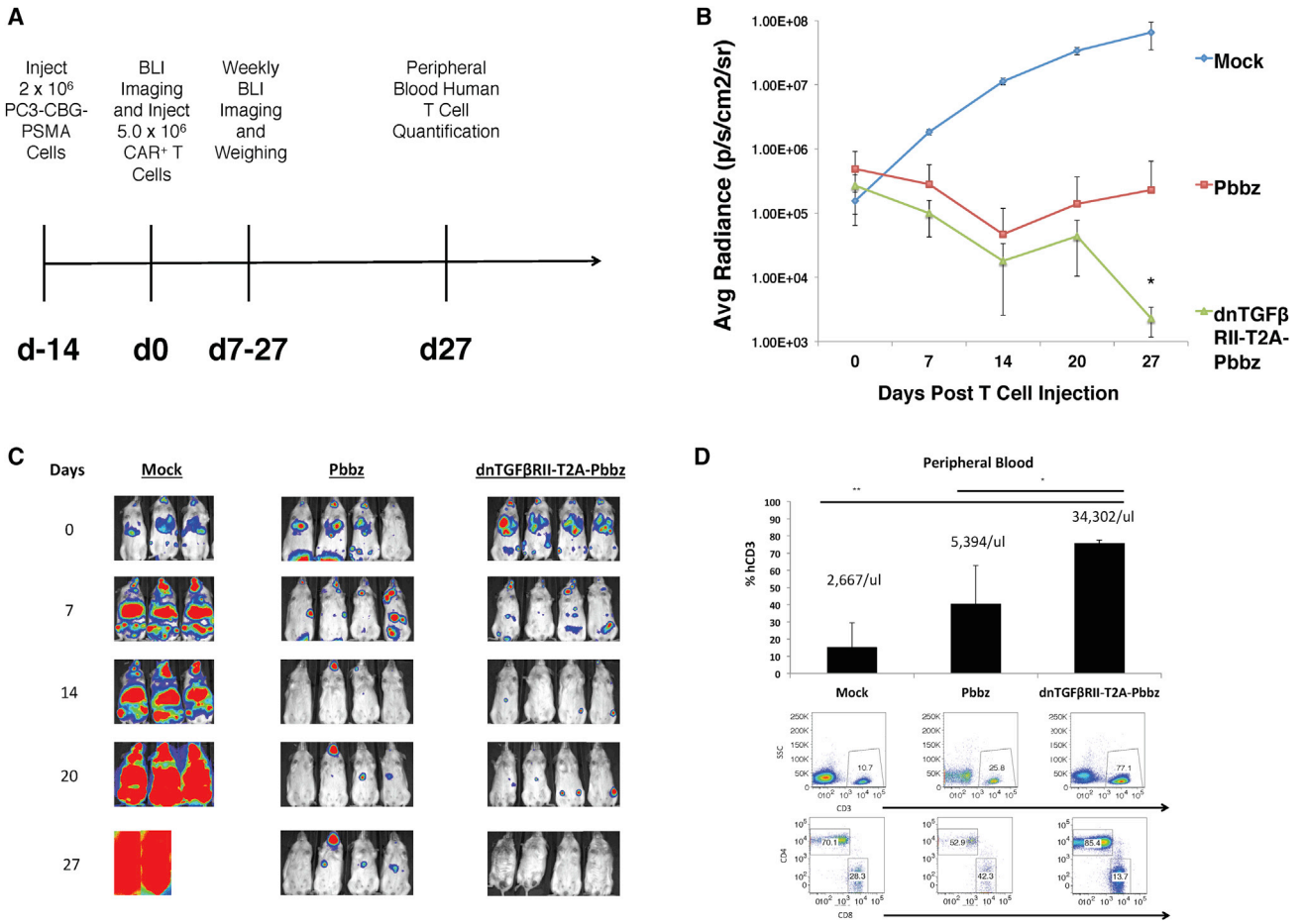

Figure 4. dnTGF-βRII-T2A-Pbbz CAR T Cells Have Augmented Proliferation and Eradicate Metastatic Prostate Cancer *In Vivo*

Systemic PC3-PSMA tumors were established by tail vein infusions of 2×10^6 tumor cells with the timeline described in (A) treated by infusing 5.0×10^6 CAR T cells or PBS (mock) per mouse 2 weeks later. Mice were assessed with bioluminescent imaging (BLI) weekly to assess tumor burden (B). Images of this BLI assessment are shown to demonstrate location and burden of tumors (C). Mice were bled at the end of the experiment at day 27 to assess the phenotype and the amounts of human CD3 T cells within the blood of these mice (D) (n = 4 mice/group). The error bars represent ± SD. *p < 0.05 and **p < 0.01, determined using a Student's two-tailed t test.

expected to enhance innate and acquired immunity. The cytokine profile demonstrates a balanced T_H2 phenotype with IL-4, IL-5, and IL-13 expression, as well as T_H1 phenotype with IL-2; IFN-γ; and chemokines MIP1-α, MIP1-β, and RANTES. In previous studies, CD4+ T cells and tumor cells engineered to secrete IL-4 have been shown to have potent antitumor effects.[31,32]

In addition to enhanced cytokine secretion, we identified the expression of a major network of genes associated with cell cycle progression and cell division, as well as increased expression of transcription factors associated with robust T cell effector functions. The pronounced differential expression of cell cycle genes was late to emerge after 21 days of culture. It is possible that this simply reflects continued proliferation of the dnTGF-βRII-T2A-Pbbz CAR T cells, while the PSMA Pbbz CAR T cells become progressively exhausted with decreased proliferation. Previous studies have reported that chronic stimulation of CAR T cells can lead to exhaustion, terminal differentiation, and apoptosis.[33,34] It is noteworthy that enhanced proliferation of the dnTGF-βRII-T2A-Pbbz CAR T cells was observed consistently *in vitro* and in all 3 *in vivo* experiments.

A third mechanism identified that may contribute to enhanced antitumor efficacy was a reduction of $CD4^+FoxP3^+$ cells that was observed after 21 days of co-culture with PC3-PSMA tumor cells. Along with an increase of $CD4^+$ central memory and $CD127^+$ T cells, these effects would be expected to contribute to enhanced CAR T cell proliferation.[35]

From the three animal experiments, it is evident that the dnTGF-βRII allows for enhanced antitumor responses when using the Pbbz CAR, allowing for tumor eradication and sustained long-term proliferation and persistence of the T cells. We found that the dnTGF-βRII gave much higher numbers of human T cells within the blood of these mice, correlating with substantial weight loss and GVHD. Most of

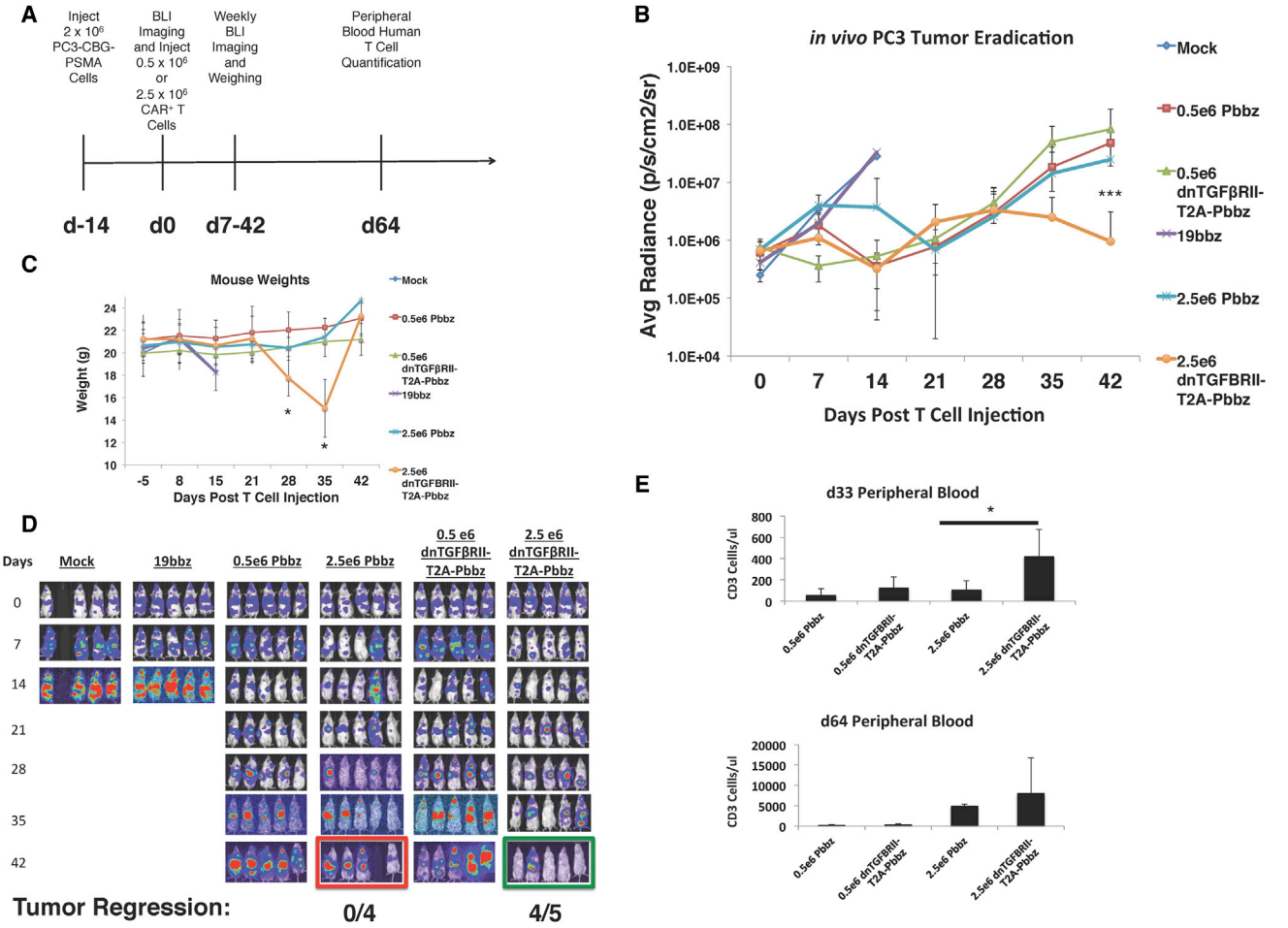

Figure 5. Dose-Dependent Augmentation of CAR T Cell Proliferation and Antitumor Efficacy of dnTGF-βRII CAR T Cells Compared to PSMA CAR T Cells *In Vivo*

Systemic PC3-PSMA tumors were established from intravenous (i.v.) infusions with the timeline described in (A), with varied doses of 0.5×10^6 and 2.5×10^6 CAR T cells per mouse infused 2 weeks later. Mice were assessed with BLI weekly to assess tumor burden (B). Body weight of the groups of mice is shown in (C). Images of this BLI assessment are shown to demonstrate location and burden of tumors (D). Mice were bled at days 33 and 64 to assess the amounts of human CD3 T cells within the blood of these mice (E) (n = 5 mice/group). The error bars represent ± SD. *$p < 0.05$ and ***$p < 0.001$.

the T cells were skewed to $CD4^+$ *in vivo*. Significantly higher amounts of $CD8^+$ central memory cells were observed with the dnTGF-βRII-T2A-Pbbz group. These toxic effects of the dnTGF-βRII-T2A-Pbbz CAR T cells are most likely due to enhanced xenogeneic effector functions of the CAR T cells.

A limitation of our approach is that the enhanced proliferation of the dnTGF-βRII-T2A-Pbbz CAR T cells could lead to a lymphoproliferative syndrome, as has been reported in mice.[20] To date, we have not observed antigen or growth factor-independent proliferation of dnTGF-βRII-T2A-Pbbz CAR T cells. A recent study has shown that mouse T cells can transform if haploinsufficient for PD-1.[36] It is possible that TGF-β has a similar cell-intrinsic tumor suppressor function in T cells. The immunodeficient mouse models that we and others in the field use have not generally predicted toxicities of CAR T cells, such as cytokine release syndrome or neurologic toxicity.[37–39]

Based on these encouraging preclinical results, we have initiated a clinical trial to infuse dnTGF-βRII-T2A-PBBZ CAR T cells in a first-in-human study in patients with refractory castration-resistant metastatic prostate cancer (ClinicalTrials.gov: NCT03089203). Through these investigations, we hope to learn better methods to sustain and augment CAR T cell proliferation and effector function in patients with advanced solid tumors.

MATERIALS AND METHODS

Vector Design

mRNA was isolated using the RNEasy Plus Mini Kit (QIAGEN) from human peripheral blood mononuclear cells (PBMCs) to produce

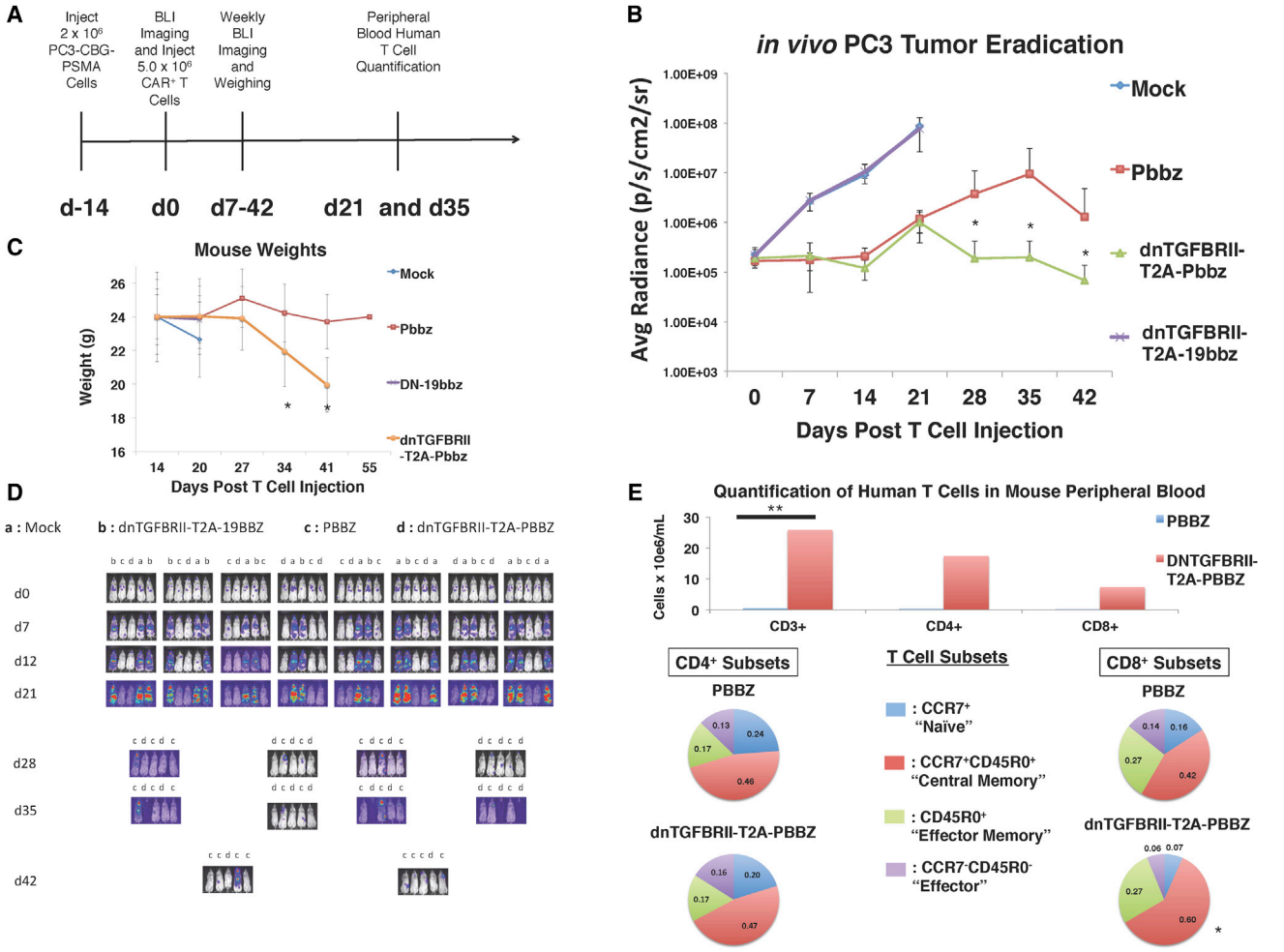

Figure 6. Enhanced Survival and Central Memory PSMA dnTGF-βRII-T2A-Pbbz CAR T Cells *In Vivo* in Mice with Metastatic Prostate Cancer

Systemic PC3-PSMA tumors were established by tail vein infusion with the timeline described in (A) with a dose of 5.0 × 10^6 CAR T cells per mouse infused 2 weeks later. Mice were assessed with BLI weekly to assess tumor burden (B). Body weight is shown in (C) and images of this BLI assessment are shown to demonstrate location and burden of tumors (D). (E) Mice were bled at the end of the experiment at day 35 to assess the amounts of human $CD3^+$ T cells within the blood of these mice. In depth analysis to assess T cell subsets was performed based on memory markers (CCR7, CD45R0, and CD127) (n = 10 mice/group). The error bars represent ± SD. *$p < 0.05$ and **$p < 0.01$.

cDNA using RETROscript cDNA kit (Ambion). Primers were designed to amplify the TGF-βRII transcript variant 2 (NM_003242), including a 5′ BspEI site and a 3′ NheI site. This was cloned into pELNS-tetR-T2A-Zeocin to replace the tetR cistron to form pELNS-TGF-βRII-T2A-Zeocin. Next, the TGF-βRII-T2A-Zeocin cassette was moved into the lentiviral expression plasmid from the Translational Research Program (pTRPE) lentiviral vector under the EF1alpha promoter utilizing the XbaI and SalI sites. A CAR was designed and synthesized by Geneart (Thermo Fisher Scientific) utilizing the variable light and heavy chains of the J591 antibody sequence from Dr. Neil Bander's (Weill Cornell Medical College) patent application (WO2002098897A2), fused to the 4-1BB intracellular domain sequence and CD3ζ intracellular domain sequences.[40] The dominant-negative TGF-βRII was constructed by truncating the human TGFBRII to remove the intracellular kinase domain at residue 199 as originally reported.[17] Synthesized CAR DNA was digested with XbaI and SalI and inserted into pTRPE-TGF-βRII-T2A-Zeocin utilizing the Avr2 and SalI sites.

Lentiviral Vector Production and CAR T Cell Production

Lentiviral supernatants were collected from tripartite-transfected HEK293T cells and concentrated using ultracentrifugation, as described by Resier et al.[41] These lentiviral vectors were used to transduce normal donor human T cells isolated from PBMCs using anti-CD4 and anti-CD8 microbeads (Miltenyi Biotec) and activated for 24 hr with anti-CD3/CD28 Dynabeads (Thermo Fisher Scientific). Transduced T cells were expanded for around 9 days in R10 media consisting of RPMI media (Gibco) with 10% fetal bovine serum

(FBS) (HyClone), 4-(2-hydroxyethyl)-1-piperazineethanesulfonic acid (HEPES), penicillin, and streptomycin with 30 U/mL IL-2. CAR T cells were then cryopreserved in 90% FBS and 10% DMSO for future use.

Cell Lines

The PC3 prostate cancer cell line, obtained from ATCC (CRL-1435), was isolated from a bone metastasis of a 62-year-old Caucasian with grade IV adenocarcinoma of the prostate. These cells grow to confluency *in vitro* within 3–4 days of being seeded at 1×10^4 cells/cm^2 and cultured in D10 media consisting of DMEM with 10% FBS (HyClone), HEPES, penicillin, and streptomycin. The tumor cell line was regularly validated to be Mycoplasma free, and it was authenticated in 2016 by the University of Arizona Genetics Core (Tucson, AZ). Using pTRPE vectors, we transduced these PC3 cells with lentiviral vectors to express click beetle green luciferase with GFP for easy quantification of lysis and *in vivo* tumor burden. We then used another pTRPE lentiviral vector to introduce the PSMA protein into these cells. These PC3 cells were sorted to 99% purity for the desired vectors using a BD FACS Aria II.

Flow Cytometry

A 4-laser LSRFortessa and a LSRII (Becton Dickinson) flow cytometer were used for analysis. Cells were stained in fluorescence-activated cell sorting (FACS) buffer (0.5% BSA Fraction V [Sigma], 2 mM EDTA [Life Technologies], in PBS [Life Technologies]) at 4°C for 30 min with the appropriate antibodies. For surface detection of the CAR, we used Jackson Laboratories Goat-anti-mouse PE-conjugated F(ab')2 (115-116-072) antibody. The R&D Systems TGF-βRII antibody antigen-presenting cell (APC) conjugate (FAB2411A) was used to detect the dnTGF-βRII. To detect phosphor-SMAD2/3, we used BD Phosflow antibodies (562586) with the recommended intracellular staining products and protocols (BD Biosciences). The following antibodies were used for T cell phenotyping: CD3-BV605, CD4-BV510, CD127-BV711 (BioLegend), CCR7-FITC, CD8-APCH7, CD45RO-PE (Becton Dickinson), FoxP3-PE, and Helios-PerCP-Cy5.5 (eBiosciences). For FoxP3 and Helios staining, the recommended intranuclear staining products and protocols were used (eBiosciences). To process mouse blood for flow cytometry, 50 of 65 μL blood retroorbitally drawn was lysed on ice for 5 min with 2 mL 1× RBC Lysis Buffer (BioLegend), centrifuged at 4°C for 5 min at 500 × *g*, washed twice with FACS buffer, and used for antibody staining. Countbright beads (Thermo Fisher Scientific) were used to determine the absolute number of cells per milliliter of blood.

TGF-β ELISA

To reduce the amount of background TGF-β present in FBS, we serum starved these cells at 0.5% FBS in order to determine the amount of TGF-β truly secreted by the tumor cell lines. Cells were cultured at 1e6 cells/well in 6-well plates for 24 hr and supernatants were harvested. To determine the amount of latent TGF-β secreted by tumor cell lines, the TGF-β ELISA kit (R&D Systems, DY240-05) was used to quantify the amount of TGF-β present in the supernatant. Undetectable amounts of mature TGF-β were observed, so supernatant samples were treated for 10 min at room temperature (RT) with 1N HCL and neutralized with 1N NaOH with 0.5 M HEPES to cleave latent TGF-β into mature TGF-β.

Tumor Lysis Assays

Since our PC3 cells were designed to express luciferase, the Promega Luciferase Reporter Assay System (E1910) was used to correlate luminescence to percentage cell lysis. By including tumor cells alone as 0% lysis and by completely lysing them in 0.01% Triton X-100 as 100% lysis, we established a sensitive method to detect percentage lysis of tumor cells by CAR T cells. After 16 hr of co-culture of PC3 cells with T cells at effector:target ratios from 0 to 25:1, cells were harvested, lysed, and luminescence was determined using the Promega system.

T Cell *In Vitro* Proliferation Assay

PC3 cells were irradiated with 15 Gy irradiation and plated at 0.2e6 cells per well of 12-well plates. 24 hr later, 1e6 T cells total were plated with the irradiated PC3 cells in R10 media without any IL-2 added in 2 mL media. Media were added as necessary, usually 4 days after plating if cell densities were over 1e6/mL and media were yellowing for 4 mL media/well total. 1e6 T cells from these cultures were taken and replated on freshly irradiated 0.2e6 PC3 cells, and this assay was continued with replating T cells on irradiated tumor cells every week. Cell numbers and size were evaluated using a Beckman Coulter Multisizer 3 Cell Counter.

Cytokine Analysis

Using the harvested supernatants 24 hr after plating co-cultures from these long-term proliferation assays, the human cytokine magnetic 30-Plex panel (Life Technologies LHC6003M) was used to quantify the following cytokines: IL-1RA, fibroblast growth factor (FGF)-basic, MCP-1, granulocyte colony-stimulating factor [G-CSF], IFN-γ, IL-12, IL-13, IL-7, granulocyte-macrophage colony-stimulating factor [GM-CSF], TNF-α, IL-1β, IL-2, IL-4, IL-5, IL-6, IFN-α, IL-15, IL-10, macrophage inflammatory protein [MIP]-1α, IL-17, IL-8, epidermal growth factor (EGF), human growth factor [HGF], vascular endothelial growth factor [VEGF], monokine induced by gamma IFN [MIG], RANTES, Eotaxin, MIP-1β, IFN-γ-induced protein 10 [IP-10], and IL-2R. Samples were measured on a FlexMAP 3D instrument (Luminex, Austin, TX) and evaluated with xPONENT software (Luminex).

Global Gene Expression Profiling

Live cells were isolated from the long-term proliferation cultures using a dead cell removal kit (Miltenyi 130-090-101), and whole RNA was isolated using RNeasy Mini Isolation Kit (QIAGEN 74104). These samples were isolated in triplicate at multiple time points and were submitted to the Molecular Profiling Core Facility at the University of Pennsylvania. These samples were run on Human GeneChip Microarray 2.0 ST microarrays (Thermo Fisher Scientific), and analysis was performed using Transcriptome and Expression Analysis Console (Thermo Fisher Scientific). DEGs that were significant ($p < 0.05$) were uploaded into STRING version (v.)10.5 *Homo*

sapiens,[27] which clusters genes into networks based on scored interactions, associations, and pathway knowledge drawn from databases such as KEGG and Gene Ontology and text mined from PubMed literature. Networks were constructed where the network edges were based on a minimum interaction confidence of 0.4, a maximum of 10 interactors, and the interaction sources were as follows: text-mining, experiments, databases, co-expression, neighborhood, gene fusion, and co-occurrence.

Animal Experiments

The University of Pennsylvania Institutional Animal Care and Use Committee approved all animal experiments. Female NSG knockout (KO) mice were provided and housed by the University of Pennsylvania Stem Cell and Xenograft core. Using 200 μL 1× PBS, 2e6 PC3-PSMA cells were injected intravenously via the tail vein. Tumors were established systemically for 2 weeks, upon which CAR T cells were then injected at various doses in the same manner. Bioluminescence imaging was performed by injecting mice weekly intraperitoneally with luciferin and quantifying luminescence using a Xenogen IVIS-200 Spectrum imaging system. Blood was drawn using glass capillary tubes from the retroorbital sinus. All experiments were performed via protocols approved by the Institutional Animal Care and Use Committee of the University of Pennsylvania.

Statistics

All statistical analysis was performed using GraphPad Prism v.6 (GraphPad Software Inc.). For comparisons of 2 groups, 2-tailed unpaired t tests were used. Correlation was estimated by calculation of 2-tailed Pearson coefficients and significance. Data were transformed when needed to normalize variance. Power analysis was conducted using software as reported.[42] Symbols indicate statistical significance as follows: *$p < 0.05$, **$p < 0.01$, and ***$p < 0.005$.

SUPPLEMENTAL INFORMATION

Supplemental Information includes one figure and three tables and can be found with this article online at https://doi.org/10.1016/j.ymthe.2018.05.003.

AUTHOR CONTRIBUTIONS

C.C.K. designed and performed experiments, analyzed data, interpreted results, and wrote the manuscript. J.L. contributed reagents, designed and performed experiments, and analyzed data. A.Z. and F.C. performed experiments. J.J.M. and S.F.L. designed experiments, interpreted results, and edited the manuscript. M.V.M. and Y.Z. designed experiments and interpreted results. J.A.F. contributed reagents, designed and performed experiments, analyzed data, interpreted results, and edited the manuscript. C.H.J. designed experiments, analyzed data, interpreted results, and wrote the manuscript.

CONFLICTS OF INTEREST

Y.Z. submitted a patent application related to this work. The authors have sponsored research support from Tmunity.

ACKNOWLEDGMENTS

This work was supported by grants from the Prostate Cancer Foundation to M.V.M., Y.Z., and C.H.J. and Young Investigator Awards to C.C.K. and J.L.

REFERENCES

1. Litwin, M.S., and Tan, H.J. (2017). The Diagnosis and Treatment of Prostate Cancer: A Review. JAMA *317*, 2532–2542.
2. Kwon, E.D., Drake, C.G., Scher, H.I., Fizazi, K., Bossi, A., van den Eertwegh, A.J., Krainer, M., Houede, N., Santos, R., Mahammedi, H., et al.; CA184-043 Investigators (2014). Ipilimumab versus placebo after radiotherapy in patients with metastatic castration-resistant prostate cancer that had progressed after docetaxel chemotherapy (CA184-043): a multicentre, randomised, double-blind, phase 3 trial. Lancet Oncol. *15*, 700–712.
3. Chen, D.S., and Mellman, I. (2017). Elements of cancer immunity and the cancer-immune set point. Nature *541*, 321–330.
4. Huang, A.C., Postow, M.A., Orlowski, R.J., Mick, R., Bengsch, B., Manne, S., Xu, W., Harmon, S., Giles, J.R., Wenz, B., et al. (2017). T-cell invigoration to tumour burden ratio associated with anti-PD-1 response. Nature *545*, 60–65.
5. Verdegaal, E.M., de Miranda, N.F., Visser, M., Harryvan, T., van Buuren, M.M., Andersen, R.S., Hadrup, S.R., van der Minne, C.E., Schotte, R., Spits, H., et al. (2016). Neoantigen landscape dynamics during human melanoma-T cell interactions. Nature *536*, 91–95.
6. June, C.H., Warshauer, J.T., and Bluestone, J.A. (2017). Is autoimmunity the Achilles' heel of cancer immunotherapy? Nat. Med. *23*, 540–547.
7. Sadelain, M., Rivière, I., and Riddell, S. (2017). Therapeutic T cell engineering. Nature *545*, 423–431.
8. Lim, W.A., and June, C.H. (2017). The Principles of Engineering Immune Cells to Treat Cancer. Cell *168*, 724–740.
9. Rabinovich, G.A., Gabrilovich, D., and Sotomayor, E.M. (2007). Immunosuppressive strategies that are mediated by tumor cells. Annu. Rev. Immunol. *25*, 267–296.
10. Joyce, J.A., and Fearon, D.T. (2015). T cell exclusion, immune privilege, and the tumor microenvironment. Science *348*, 74–80.
11. Chong, E.A., Melenhorst, J.J., Lacey, S.F., Ambrose, D.E., Gonzalez, V., Levine, B.L., June, C.H., and Schuster, S.J. (2017). PD-1 blockade modulates chimeric antigen receptor (CAR)-modified T cells: refueling the CAR. Blood *129*, 1039–1041.
12. Condomines, M., Arnason, J., Benjamin, R., Gunset, G., Plotkin, J., and Sadelain, M. (2015). Tumor-Targeted Human T Cells Expressing CD28-Based Chimeric Antigen Receptors Circumvent CTLA-4 Inhibition. PLoS ONE *10*, e0130518.
13. Siegel, P.M., and Massagué, J. (2003). Cytostatic and apoptotic actions of TGF-β in homeostasis and cancer. Nat. Rev. Cancer *3*, 807–821.
14. Hanahan, D., and Weinberg, R.A. (2011). Hallmarks of cancer: the next generation. Cell *144*, 646–674.
15. Travis, M.A., and Sheppard, D. (2014). TGF-β activation and function in immunity. Annu. Rev. Immunol. *32*, 51–82.
16. Ebner, R., Chen, R.H., Shum, L., Lawler, S., Zioncheck, T.F., Lee, A., Lopez, A.R., and Derynck, R. (1993). Cloning of a type I TGF-beta receptor and its effect on TGF-beta binding to the type II receptor. Science *260*, 1344–1348.
17. Wieser, R., Attisano, L., Wrana, J.L., and Massagué, J. (1993). Signaling activity of transforming growth factor beta type II receptors lacking specific domains in the cytoplasmic region. Mol. Cell. Biol. *13*, 7239–7247.
18. Gorelik, L., and Flavell, R.A. (2001). Immune-mediated eradication of tumors through the blockade of transforming growth factor-beta signaling in T cells. Nat. Med. *7*, 1118–1122.
19. Gorelik, L., and Flavell, R.A. (2000). Abrogation of TGFbeta signaling in T cells leads to spontaneous T cell differentiation and autoimmune disease. Immunity *12*, 171–181.
20. Lucas, P.J., Kim, S.J., Melby, S.J., and Gress, R.E. (2000). Disruption of T cell homeostasis in mice expressing a T cell-specific dominant negative transforming growth factor beta II receptor. J. Exp. Med. *191*, 1187–1196.

21. Zhang, Q., Yang, X., Pins, M., Javonovic, B., Kuzel, T., Kim, S.J., Parijs, L.V., Greenberg, N.M., Liu, V., Guo, Y., and Lee, C. (2005). Adoptive transfer of tumor-reactive transforming growth factor-beta-insensitive CD8+ T cells: eradication of autologous mouse prostate cancer. Cancer Res. *65*, 1761–1769.

22. Donkor, M.K., Sarkar, A., Savage, P.A., Franklin, R.A., Johnson, L.K., Jungbluth, A.A., Allison, J.P., and Li, M.O. (2011). T cell surveillance of oncogene-induced prostate cancer is impeded by T cell-derived TGF-β1 cytokine. Immunity *35*, 123–134.

23. Foster, A.E., Dotti, G., Lu, A., Khalil, M., Brenner, M.K., Heslop, H.E., Rooney, C.M., and Bollard, C.M. (2008). Antitumor activity of EBV-specific T lymphocytes transduced with a dominant negative TGF-beta receptor. J. Immunother. *31*, 500–505.

24. Bollard, C.M., Tripic, T., Cruz, C.R., Dotti, G., Gottschalk, S., Torrano, V., Dakhova, O., Carrum, G., Ramos, C.A., Liu, H., et al. (2018). Tumor-Specific T-Cells Engineered to Overcome Tumor Immune Evasion Induce Clinical Responses in Patients With Relapsed Hodgkin Lymphoma. J. Clin. Oncol. *36*, 1128–1139.

25. Vallabhajosula, S., Nikolopoulou, A., Jhanwar, Y.S., Kaur, G., Tagawa, S.T., Nanus, D.M., Bander, N.H., and Goldsmith, S.J. (2016). Radioimmunotherapy of Metastatic Prostate Cancer with ^{177}Lu-DOTAhuJ591 Anti Prostate Specific Membrane Antigen Specific Monoclonal Antibody. Curr. Radiopharm. *9*, 44–53.

26. Bander, N.H., Trabulsi, E.J., Kostakoglu, L., Yao, D., Vallabhajosula, S., Smith-Jones, P., Joyce, M.A., Milowsky, M., Nanus, D.M., and Goldsmith, S.J. (2003). Targeting metastatic prostate cancer with radiolabeled monoclonal antibody J591 to the extracellular domain of prostate specific membrane antigen. J. Urol. *170*, 1717–1721.

27. Szklarczyk, D., Franceschini, A., Wyder, S., Forslund, K., Heller, D., Huerta-Cepas, J., Simonovic, M., Roth, A., Santos, A., Tsafou, K.P., et al. (2015). STRING v10: protein-protein interaction networks, integrated over the tree of life. Nucleic Acids Res. *43*, D447–D452.

28. Beretta, E., Dhillon, H., Kalra, P.S., and Kalra, S.P. (2002). Central LIF gene therapy suppresses food intake, body weight, serum leptin and insulin for extended periods. Peptides *23*, 975–984.

29. Kalos, M., Levine, B.L., Porter, D.L., Katz, S., Grupp, S.A., Bagg, A., and June, C.H. (2011). T cells with chimeric antigen receptors have potent antitumor effects and can establish memory in patients with advanced leukemia. Sci. Transl. Med. *3*, 95ra73.

30. Ali, S.A., Shi, V., Maric, I., Wang, M., Stroncek, D.F., Rose, J.J., Brudno, J.N., Stetler-Stevenson, M., Feldman, S.A., Hansen, B.G., et al. (2016). T cells expressing an anti-B-cell maturation antigen chimeric antigen receptor cause remissions of multiple myeloma. Blood *128*, 1688–1700.

31. Golumbek, P.T., Lazenby, A.J., Levitsky, H.I., Jaffee, L.M., Karasuyama, H., Baker, M., and Pardoll, D.M. (1991). Treatment of established renal cancer by tumor cells engineered to secrete interleukin-4. Science *254*, 713–716.

32. Hung, K., Hayashi, R., Lafond-Walker, A., Lowenstein, C., Pardoll, D., and Levitsky, H. (1998). The central role of CD4(+) T cells in the antitumor immune response. J. Exp. Med. *188*, 2357–2368.

33. Long, A.H., Haso, W.M., Shern, J.F., Wanhainen, K.M., Murgai, M., Ingaramo, M., Smith, J.P., Walker, A.J., Kohler, M.E., Venkateshwara, V.R., et al. (2015). 4-1BB costimulation ameliorates T cell exhaustion induced by tonic signaling of chimeric antigen receptors. Nat. Med. *21*, 581–590.

34. Frigault, M.J., Lee, J., Basil, M.C., Carpenito, C., Motohashi, S., Scholler, J., Kawalekar, O.U., Guedan, S., McGettigan, S.E., Posey, A.D., Jr., et al. (2015). Identification of chimeric antigen receptors that mediate constitutive or inducible proliferation of T cells. Cancer Immunol. Res. *3*, 356–367.

35. Lee, J.C., Hayman, E., Pegram, H.J., Santos, E., Heller, G., Sadelain, M., and Brentjens, R. (2011). In vivo inhibition of human CD19-targeted effector T cells by natural T regulatory cells in a xenotransplant murine model of B cell malignancy. Cancer Res. *71*, 2871–2881.

36. Wartewig, T., Kurgyis, Z., Keppler, S., Pechloff, K., Hameister, E., Öllinger, R., Maresch, R., Buch, T., Steiger, K., Winter, C., et al. (2017). PD-1 is a haploinsufficient suppressor of T cell lymphomagenesis. Nature *552*, 121–125.

37. Gust, J., Hay, K.A., Hanafi, L.A., Li, D., Myerson, D., Gonzalez-Cuyar, L.F., Yeung, C., Liles, W.C., Wurfel, M., Lopez, J.A., et al. (2017). Endothelial Activation and Blood-Brain Barrier Disruption in Neurotoxicity after Adoptive Immunotherapy with CD19 CAR-T Cells. Cancer Discov. *7*, 1404–1419.

38. Fitzgerald, J.C., Weiss, S.L., Maude, S.L., Barrett, D.M., Lacey, S.F., Melenhorst, J.J., Shaw, P., Berg, R.A., June, C.H., Porter, D.L., et al. (2017). Cytokine Release Syndrome After Chimeric Antigen Receptor T Cell Therapy for Acute Lymphoblastic Leukemia. Crit. Care Med. *45*, e124–e131.

39. Maude, S., and Barrett, D.M. (2016). Current status of chimeric antigen receptor therapy for haematological malignancies. Br. J. Haematol. *172*, 11–22.

40. Milone, M.C., Fish, J.D., Carpenito, C., Carroll, R.G., Binder, G.K., Teachey, D., Samanta, M., Lakhal, M., Gloss, B., Danet-Desnoyers, G., et al. (2009). Chimeric receptors containing CD137 signal transduction domains mediate enhanced survival of T cells and increased antileukemic efficacy in vivo. Mol. Ther. *17*, 1453–1464.

41. Kutner, R.H., Zhang, X.Y., and Reiser, J. (2009). Production, concentration and titration of pseudotyped HIV-1-based lentiviral vectors. Nat. Protoc. *4*, 495–505.

42. Dupont, W.D., and Plummer, W.D., Jr. (1998). Power and sample size calculations for studies involving linear regression. Control. Clin. Trials *19*, 589–601.